(3) F. A. Cotton, *Inorg. Chem.*, **4**, 334 (1965).
(4) F. A. Cotton, N. F. Curtis and W. R. Robinson, *Inorg. Chem.*, **4**, 1696 (1965).
(5) F. A. Cotton, C. Oldham, and R. A. Walton, *Inorg. Chem.*, **6**, 214 (1967).
(6) M. J. Bennett, F. A. Cotton, and R. A. Walton, *J. Am. Chem. Soc.*, **88**, 3866 (1966).
(7) M. J. Bennett, F. A. Cotton, and R. A. Walton, *Proc. R. Soc. London, Ser. A*, **303**, 175 (1968).
(8) M. J. Bennett, F. A. Cotton, B. M. Foxman, and P. F. Stokely, *J. Am. Chem. Soc.*, **89**, 2759 (1967).
(9) F. A. Cotton and B. M. Foxman, *Inorg. Chem.*, **7**, 2135 (1968).
(10) (a) J. R. Ebner and R. A. Walton, *Inorg. Chem.*, **14**, 1987 (1975); (b) R. A. Walton, private communications.
(11) F. A. Cotton, B. A. Frenz, J. R. Ebner, and R. A. Walton, *J. Chem. Soc., Chem. Commun.*, 4 (1974); *Inorg. Chem.*, **15**, 1630 (1976).
(12) F. A. Cotton and J. M. Troup, *J. Am. Chem. Soc.*, **96**, 4422 (1974).
(13) A. B. Brignole and F. A. Cotton, *Inorg. Synth.*, **13**, 82 (1972).
(14) DATARED by Frenz was used for data reduction. AGNOST, used for the absorption correction, is a modification by Frenz of Cohen's AGNOST. The Fourier program JIMDP by Ibers is a version of Zalkin's FORDAP. NUCLS, a full-matrix least-squares program by Ibers and Doedens, closely resembles Busing and Levy's ORFLS program; the function minimized in the refinement is $\sum w(|F_o| - |F_c|)^2$. ORTEP by Johnson was used for drawing illustrations on a Gerber plotter. Atomic distances, angles, and errors were calculated using program ORFFE by Busing, Martin, and Levy as modified by Brown, Johnson, and Thiessen.
(15) D. T. Cromer and D. Liberman, *J. Chem. Phys.*, **53**, 1891 (1971).
(16) D. T. Cromer and J. T. Waber, "International Tables for X-Ray Crystallography", Vol. IV, Kynoch Press, Birmingham, England, 1974, Table 2.3.1.
(17) Supplementary material.
(18) F. A. Cotton and L. W. Shive, *Inorg. Chem.*, **14**, 2027 (1975).

Contribution from the Departments of Chemistry, Texas A&M University, College Station, Texas 77843, and Princeton University, Princeton, New Jersey 08540

The Tungsten–Tungsten Triple Bond. 3. Dimethyltetrakis(diethylamido)ditungsten. Structure and Dynamical Solution Behavior

M. H. CHISHOLM,*[1a] F. A. COTTON,*[1b] M. EXTINE,[1a] M. MILLAR,[1b] and B. R. STULTS[1b]

Received March 22, 1976 AIC60200T

The title compound, $(Et_2N)_2MeW{\equiv}WMe(NEt_2)_2$, has been prepared and thoroughly characterized by means of x-ray crystallography, by carbon-13 NMR over the temperature range −60 to +60 °C, and by other physical and chemical methods. In solution the molecule exists as an approximately 3:2 equilibrium mixture of anti and gauche isomers. When the compound is crystallized by lowering the temperature of a concentrated solution, the solid obtained consists entirely of the anti rotamer. The crystals belong to space group $C2/c$ with unit cell parameters a = 17.033 (5) Å, b = 8.258 (2) Å, c = 18.817 (4) Å, and β = 103.34 (2)°. The molecules are located on centers of symmetry and have the following important dimensions: W–W = 2.288 Å, W–N(mean) = 1.966 Å, W–C = 2.171 Å, W–W–C = 101.6°, W–W–N = 104.2°. The ^{13}C NMR spectra allowed us to observe the following dynamic properties. At equilibrium in toluene solution the g:a (gauche:anti) ratio is about 3:2 at all temperatures from −60 to +60 °C. Even at +60 °C the rate of g $\rightleftharpoons$ a interconversion is too small to influence line shapes. The activation energy for this process is estimated to be about 21 kcal mol^{-1}. Internal rotations about the W–N bonds allow interchange of the proximal and distal ethyl groups. The activation energies for the two types in the gauche rotamer differ by about 2.5 kcal mol^{-1} while that in the anti isomer is about halfway between. A comparison of the W–C and W–N distances supports the idea that there is significant W–N π bonding.

Introduction

In earlier communications from these laboratories[2-4] and others,[5] the existence of an extensive chemistry of dinuclear compounds containing triply bonded pairs of molybdenum and tungsten atoms has been indicated. We have prepared and characterized compounds containing only dialkylamide groups,[2,3] viz., $M_2(NR_2)_6$, as well as those containing a mixture of NR_2 groups and halogen atoms,[4] e.g., $W_2(NEt_2)_4Cl_2$. Wilkinson[5] had shown that pure alkyls (of the type incapable of β elimination, e.g., $M_2(CH_2SiMe_3)_6$) can be prepared.[6]

In this paper we describe a compound which connects the amido series with the organo series, namely, the mixed amido–alkyl species $W_2Me_2(NEt_2)_4$.

Experimental Section

Preparation. A procedure for the preparation of $W_2Me_2(NEt_2)_4$ has been given in an earlier paper.[4] However, we have since found that the following modification of that procedure gives better results. All operations are conducted in an N_2 atmosphere.

Methyllithium (9.0 mmol) in ether (6 ml) was added dropwise to a stirred solution of $W_2Cl_2(NEt_2)_4$ (2.19 g; 3.0 mmol) in ether (90 ml) at 25 °C. Stirring was continued for 60 min while a white precipitate appeared. The solvent was removed under vacuum and the residue was extracted with hexane (50 ml). The filtrate was concentrated to 20 ml and cooled slowly to −20 °C. The bright red crystals were filtered and dried under vacuum. The filtrate was warmed to 50 °C, concentrated to 10 ml, and cooled to −20 °C to give an additional crop of crystals. This filtrate was again reduced to half-volume and cooled to −20 °C to give another small crop. The total yield was 1.8 g (78%). Spectral data were reported earlier.[4]

Anal. Calcd for $C_{18}H_{46}N_4W_2$: C, 31.50; H, 6.76; N, 8.16; Cl, 0.00. Found: C, 31.4; H, 6.69; N, 8.02; Cl, 0.00.

Crystal Selection and Data Collection. Crystals potentially suitable for x-ray data collection were kept immersed in heavy mineral oil in a nitrogen-filled glovebag to prevent crystal decomposition while under examination. A rectangular-shaped crystal measuring 0.225 × 0.275 × 0.400 mm was selected for collection and sealed in a thin-walled glass capillary under mineral oil. Wedging the crystal in a capillary filled with the mineral oil has proven to be the most effective means of preventing crystal decomposition during data collection. Procedures for crystal examination and characterization have been described elsewhere.[7] The crystal appeared to be of good quality on the basis of ω scans for several intense reflections, which had peak widths at half-height of 0.18–0.22°. The crystal was found to be monoclinic, with $2/m$ Laue symmetry. A small shell of data, collected at rapid scan rates for use in space group determination, having systematically absent reflections hkl ($h + k \neq 2n$) and $h0l$ ($l \neq 2n$), showed the space group to be either Cc (acentric) or $C2/c$ (centrosymmetric). Final structure refinement showed the correct space group to be $C2/c$. The final values of the lattice constants and an orientation matrix used for the calculation of setting angles in data collection were determined by least-squares refinement of the setting angles for 15 high-angle reflections, $26.0 < 2\theta(\text{Mo K}\alpha) < 36.5°$, chosen to give a good sampling of diffractometer settings and crystal indices. The refined lattice constants ($\lambda_{MoK\bar{\alpha}}$ 0.710 73 Å) are a = 17.033 (5) Å, b = 8.258 (2) Å, c = 18.817 (4) Å, β = 103.34 (2)°, and V = 2575 (1) Å^3. The observed volume was consistent with that anticipated for Z = 4, indicating that for space group $C2/c$, each molecule must lie on a crystallographic twofold axis or on an inversion center or, alternatively, that the molecules occupy general positions in space group Cc.

The data were collected at room temperature, 22 ± 2 °C, using a Syntex $P\bar{1}$ autodiffractometer equipped with a graphite-crystal monochromator, using Mo Kα radiation. Variable scan rates from 4.0 to 24.0°/min were used for symmetric θ–2θ scans from 2θ(Mo Kα$_1$) − 0.9° to 2θ(Mo Kα$_2$) + 0.9° with the ratio of total background time to total scan time equal to 0.5. A total of 2966 reflections having $0° < 2\theta(\text{Mo K}\alpha) < 55.0°$ were recorded. Three standard reflections, measured every 100 reflections, showed a uniform intensity drop of approximately 10%; thus, a linear correction for crystal decay was applied to the data. In addition, a correction for absorption was applied to all data in view of the large linear absorption coefficient of 94.68 cm^{-1}. The minimum and maximum transmission factors ranged from 0.085 to 0.185 with the average correction being 0.141. Of the 2966 data collected, 936 were rejected as being unobserved and the 2030 remaining data having $I > 3\sigma(I)$ were reduced to a set of relative $|F_o|^2$ after corrections for Lorentz and polarization effects. A value of 0.070 was used for p in the calculation of $\sigma(I)$.[7]

Structural Solution and Refinement.[8] The structure was first solved in the acentric space group *Cc*. Two cycles of full-matrix least-squares refinement, varying the positional parameters of the tungsten atoms, resulted in discrepancy indices

$$R_1 = \Sigma \| F_o | - | F_c \| / | F_o | = 0.156$$
$$R_2 = [\Sigma w(| F_o | - | F_c |)^2 / \Sigma w | F_o |^2]^{1/2} = 0.238$$

The function minimized during all least-squares refinements was $\sum w(|F_o| - |F_c|)^2$, where the weighting factor, w, equals $4F_o^2/\sigma(F_o^2)^2$. The atomic scattering factors used in all least-squares refinements were those of Cromer and Waber.[9] Anomalous dispersion effects were included in the calculated scattering factors for tungsten.[10] A difference Fourier synthesis at this point clearly revealed the positions of the 22 remaining atoms constituting the asymmetric unit in space group *Cc*. When the attempted refinement of the structural model in *Cc* resulted in poor agreement among structural parameters for equivalent portions of the molecule along with high correlation coefficients between atoms within the molecule and it was noted that the halves of the molecules appeared to be related by an inversion center located at the midpoint of the tungsten–tungsten bond, it was suspected that the correct space group is $C2/c$. A transformation was made to space group $C2/c$ by placing the center of the W–W bond on the crystallographic inversion center at 0, 0, 0. The refinement then proceeded straightforwardly. The positional parameters for the unique tungsten atom were refined to give $R_1 = 0.162$ and $R_2 = 0.225$. The 12 atoms of the asymmetric unit were refined employing isotropic temperature parameters for all atoms to $R_1 = 0.102$ and $R_2 = 0.124$. The structure was refined to convergence in four cycles of full-matrix least-squares refinement employing anisotropic thermal parameters for all atoms to give final residuals of $R_1 = 0.057$ and $R_2 = 0.071$. The final structural refinement used the 2030 reflections having $I > 3\sigma(I)$.

During the final cycle of refinement no parameter shifted by more than 0.03σ, where σ is the estimated standard deviation of that parameter. A final difference Fourier map showed no features of structural significance other than possible positions for some of the hydrogen atoms. No trends were observed in the final values of F_o and F_c as a function of Miller indices, reflection number or $\lambda^{-1} \sin\theta$. A table of observed and calculated structure factors for the data used in the final refinement is available elsewhere.[11]

NMR Spectra. Proton NMR spectra were measured on Varian HA-100 and A-60 spectrometers. Carbon-13 spectra were measured on a JEOL PFT-100/Nicolet 1080 Fourier transform spectrometer at 25.034 MHz. Temperatures are believed to be accurate to ±2 °C.

The rate of isomerization of *anti*-$W_2Me_2(NEt_2)_4$ was measured by proton NMR. About 10 mg of $W_2Me_2(NEt_2)_4$ was placed in an NMR tube. The tube was cooled with liquid N_2, and 0.5 ml of toluene-d_8 (plus HMDS) was added. The tube was then evacuated, sealed with a torch, and placed in a −78 °C bath. The $W_2(NEt_2)_4Me_2$ was dissolved by briefly removing it from the −78 °C bath and shaking it, taking care not to warm it. After all of the $W_2(NEt_2)_4Me_2$ had dissolved, the NMR tube was put into the probe of the NMR instrument, which had a temperature of 10 °C at the start of the run and 14 °C at the end. Thus, the data are all assigned an average temperature of 12 ± 2 °C. The measurement consisted in recording the height of the W–CH_3 proton peak of the gauche isomer at time intervals of several minutes. The following data [time in minutes (peak height)] were obtained: 2.5 (23), 6 (40), 7.5 (48), 10 (52), 13 (56), 19 (74), 25 (81), 31 (95), 38 (93), 45 (103). A spectrum for $t = \infty$ (118) was recorded the following day.

The absolute measurement of NMR peak heights is not highly accurate and the peak being measured is not fully resolved; thus there are both random and systematic errors in the kinetic measurement. However, a plot of the logarithm of $h_\infty/(h_\infty - h_t)$, where h_∞ is the peak height at equilibrium and h_t is the peak height at time t, gave an acceptable straight line (correlation coefficient 0.988 and error 8.6%).

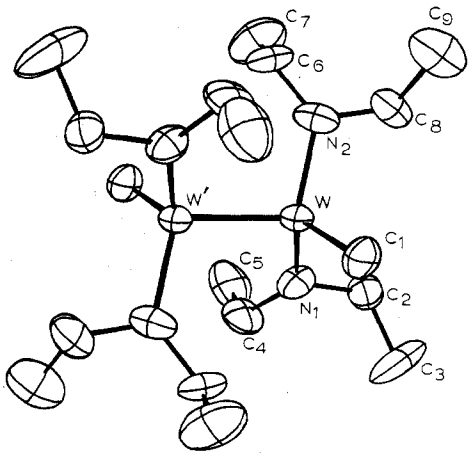

Figure 1. Molecular structure of $W_2Me_2(NEt_2)_4$ as determined crystallographically. Atoms are represented by their thermal vibration ellipsoids contoured at the 50% level and the atom numbering scheme is defined. The molecule is centrosymmetric. Unlabeled atoms have primed labels corresponding to those of the labeled atoms to which they are related by inversion.

Results and Discussion

Synthesis. A solution of $W_2Cl_2(NEt_2)_4$ in diethyl ether reacts smoothly with 2 equiv of MeLi to give $W_2Me_2(NEt_2)_4$. With less than 2 equiv of MeLi monomethylated species are formed but we have not as yet devised a satisfactory method for separating such species from $W_2Cl_2(NEt_2)_4$ and $W_2Me_2(NEt_2)_4$ which are also present in solution. With MeLi in excess of 2 equiv, $W_2Cl_2(NEt_2)_4$ reacts to give additional products which appear to be derived from NEt_2 substitution. Consequently, the reaction conditions described in the Experimental Section for the preparation of $W_2Me_2(NEt_2)_4$ should be closely followed.

$W_2Me_2(NEt_2)_4$ is a red, crystalline, diamagnetic compound. It is extremely sensitive to moisture both in the solid state and in solution (hydrocarbon solvents), but it may be stored apparently indefinitely in glass ampules in vacuo at room temperature. $W_2Me_2(NEt_2)_4$ is thermally stable below 100 °C, both in solution and in the solid. Sublimation at 100–120 °C and 10^{-4} cmHg is accompanied by considerable decomposition. In the mass spectrum a molecular ion, $W_2Me_2(NEt_2)_4^+$, is observed, together with many other W_2-containing ions.

Solid-State Structure of $W_2Me_2(NEt_2)_4$. The solid compound is composed of discrete molecules of $W_2Me_2(NEt_2)_4$ packed in a normal manner with no unusual intermolecular contacts. Each molecule has rigorous $C_i(\bar{1})$ symmetry with the midpoint of each tungsten–tungsten triple bond located on a crystallographic inversion center in space group $C2/c$. A perspective drawing showing the coordination geometry about the tungsten atoms and illustrating the atom labeling scheme is shown in Figure 1. Each of the 12 atoms in the asymmetric unit is explicitly labeled, while those atoms related by the inversion center at the midpoint of the W–W bond can be assigned the same label augmented by a single prime. The final atomic coordinates and refined anisotropic thermal parameters are given in Tables I and II, respectively. Values for the bond distances and bond angles are given in Table III.

Table I. Positional Parameters[a] for $W_2Me_2(NEt_2)_4$

	x	y	z
W	0.032 57 (3)	−0.122 32 (7)	0.008 42 (2)
N(1)	0.097 6 (6)	−0.124 0 (15)	−0.065 3 (6)
N(2)	0.085 9 (6)	−0.126 4 (17)	0.113 0 (6)
C(1)	−0.068 0 (9)	−0.290 2 (17)	−0.017 6 (8)
C(2)	0.140 3 (9)	−0.277 0 (20)	−0.067 4 (8)
C(3)	0.109 8 (14)	−0.377 7 (24)	−0.138 2 (12)
C(4)	0.115 2 (9)	−0.000 9 (21)	−0.114 3 (8)
C(5)	0.198 8 (20)	0.066 6 (25)	−0.087 8 (12)
C(6)	0.096 5 (8)	−0.002 8 (21)	0.168 6 (7)
C(7)	0.184 8 (11)	0.059 4 (27)	0.190 5 (12)
C(8)	0.127 0 (11)	−0.280 0 (22)	0.134 1 (9)
C(9)	0.096 0 (14)	−0.370 4 (28)	0.194 6 (12)

[a] Figures in parentheses are the estimated standard deviations in the least significant figures.

The structure of $W_2Me_2(NEt_2)_4$ lends itself most readily to a direct comparison with the previously reported structure[4] of $W_2Cl_2(NEt_2)_4$. The structures of the two molecules are virtually identical, and both lie on crystallographic inversion centers, although $W_2Cl_2(NEt_2)_4$ crystallizes in space group $P2_1/n$ while $W_2Me_2(NEt_2)_4$ is in space group $C2/c$. Presumably the larger van der Waals radius of the CH_3 group compared to that of the Cl atom gives rise to slightly different crystal packing forces and hence to the different space groups. The structure of $W_2Me_2(NEt_2)_4$ also merits comparison with that of $W_2(NMe_2)_6$.[3] Bond distances in the three molecules are listed in Table IV.

The entire range of variation in the W–W distances is so small that, while it may be real in a statistical sense, it does not appear to carry any chemical or electronic implications. A comparison of the W–CH_3 and W–Cl distances with the accepted covalent radii of Cl and sp^3-hybridized carbon shows a slight discrepancy, with the W–Cl distance being relatively too short. The nominal covalent radii differ by 0.22 Å while the W–Cl and W–CH_3 distances differ by only 0.16 Å. This could be the kind of effect observed long ago in compounds of nontransition elements and attributed to electronegativity differences,[12] or it may imply that there is a small amount of Cl→W π bonding.

We have previously[2-4] suggested that the W–N bonds may involve a significant amount of π character. The data in Table IV now provide direct support for that idea, via the following argument. The electronegativities of carbon and nitrogen are sufficiently similar that their bond lengths to a common third atom, W, should not be differently affected to any significant extent by ionic character. Hence, one should safely predict that a W–N pure σ bond will be shorter than the W–CH_3 bond by the difference between the covalent radii for sp^3-hybridized carbon (0.77 Å) and sp^2-hybridized nitrogen (0.67 Å). The predicted W–N single-bond length should be about 2.17 − 0.10 = 2.07 Å. In fact, the W–N bonds in all three compounds are much shorter than this, falling in the range 1.94–1.98 Å. We believe that this appreciable shortening, 0.09–0.13 Å, is attributable to N→W π bonding.

The fact that the mean W–N bond distance in $W_2Cl_2(NEt_2)_4$ is 0.03–0.04 Å shorter than in the other two compounds may be due to the greater electronegativity of Cl, which will cause the W atom to which it is attached to have a greater affinity for the π electrons of the nitrogen atoms. However,

Table II. Refined Anisotropic Thermal Parameters[a,b] for $W_2Me_2(NEt_2)_4$

	β_{11}	β_{22}	β_{33}	β_{12}	β_{13}	β_{23}
W	0.003 19 (1)	0.011 65 (6)	0.001 65 (1)	0.000 00 (7)	0.001 15 (2)	0.000 11 (6)
N(1)	0.003 5 (3)	0.015 0 (16)	0.002 8 (3)	−0.001 7 (15)	0.003 4 (4)	−0.002 0 (14)
N(2)	0.003 4 (4)	0.021 9 (22)	0.002 1 (3)	0.001 4 (19)	0.000 9 (5)	0.001 6 (16)
C(1)	0.004 1 (5)	0.011 6 (20)	0.003 2 (4)	−0.003 6 (17)	0.001 4 (7)	−0.001 2 (16)
C(2)	0.005 7 (6)	0.015 7 (22)	0.003 1 (4)	0.003 4 (20)	0.004 2 (7)	0.000 8 (17)
C(3)	0.010 7 (10)	0.030 6 (34)	0.005 8 (6)	−0.015 5 (36)	0.007 3 (13)	−0.018 5 (23)
C(4)	0.005 5 (5)	0.020 7 (27)	0.002 7 (4)	−0.000 4 (23)	0.003 8 (7)	0.004 5 (17)
C(5)	0.006 0 (7)	0.024 0 (35)	0.006 1 (8)	0.002 1 (27)	0.004 5 (11)	0.007 6 (27)
C(6)	0.004 8 (5)	0.021 7 (27)	0.001 9 (3)	−0.003 2 (24)	0.001 4 (7)	−0.004 7 (17)
C(7)	0.004 7 (7)	0.033 4 (43)	0.005 7 (8)	−0.005 4 (29)	0.001 3 (12)	−0.011 5 (30)
C(8)	0.006 2 (8)	0.019 4 (28)	0.003 1 (5)	0.002 9 (26)	0.001 6 (10)	0.005 0 (20)
C(9)	0.007 7 (10)	0.033 3 (48)	0.004 7 (7)	−0.000 6 (4)	0.002 3 (14)	0.006 9 (34)

[a] Figures in parentheses are the estimated standard deviations in the least significant digits. [b] Anisotropic thermal parameters are of the form $\exp[-(\beta_{11}h^2 + \beta_{22}k^2 + \beta_{33}l^2 + \beta_{12}hk + \beta_{13}hl + \beta_{23}kl)]$.

Table III. Bond Distances and Bond Angles[a] for $W_2Me_2(NEt_2)_4$

Distances, Å

W–W′	2.291 (1)		W–N(1)	1.965 (8)	1.967[b]
W–C(1)	2.171 (11)		W–N(2)	1.968 (9)	
N(1)–C(2)	1.462 (16)	1.453	C(2)–C(3)	1.56 (2)	1.54
–C(4)	1.449 (15)		C(4)–C(5)	1.50 (2)	
N(2)–C(6)	1.443 (15)		C(6)–C(7)	1.55 (2)	
–C(8)	1.459 (18)		C(8)–C(9)	1.55 (2)	

Bond Angles, Deg

W′–W–C(1)	101.6 (3)		N(1)–C(2)–C(3)	114 (1)	113
–N(1)	104.0 (3)	104.3	–C(4)–C(5)	112 (1)	
–N(2)	104.5 (3)		N(2)–C(6)–C(7)	112 (1)	
C(1)–W–N(1)	112.4 (4)	112.2	–C(8)–C(9)	113 (1)	
–N(2)	111.9 (4)		W(1)–N(1)–C(2)	112.9 (8)	112.3
N(1)–W–N(2)	120.1 (4)		W(1)–N(2)–C(8)	111.7 (9)	
			W(1)–N(1)–C(4)	132.7 (9)	132.2
C(2)–N(1)–C(4)	114.3 (9)	115.4	W(1)–N(2)–C(6)	131.7 (9)	
C(6)–N(2)–C(8)	116.4 (10)				

[a] Figures in parentheses are the estimated standard deviations in the least significant figures. The atom labeled W′ is related to W by the crystallographic inversion center at 0, 0, 0. [b] Averages.

Table IV. Comparison of the Bond Distances (Å) in Three Molecules Containing W–W Triple Bonds

	W–W	W–N	W–Cl	W–Me
$W_2(NMe_2)_6$[a]	2.293 (2)	1.97		
$W_2Me_2(NEt_2)_4$	2.291 (1)	1.967 (10)		2.171 (11)
$W_2Cl_2(NEt_2)_4$	2.302 (1)	1.936 (10)	2.332 (8)	

[a] Distances reported for $W_2(NMe_2)_6$ are the averaged values from the two separate structure determinations (see ref 3).

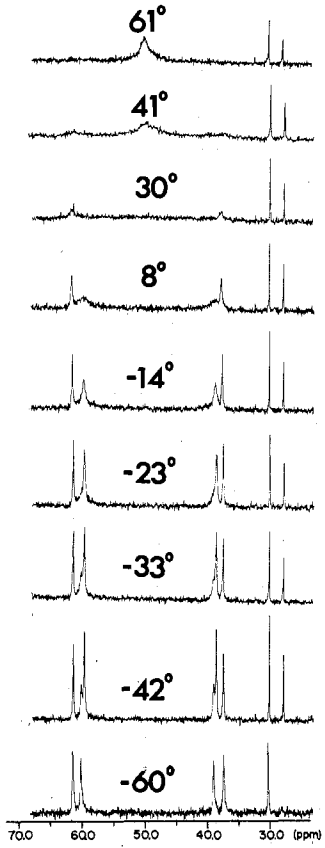

Figure 2. Carbon-13 NMR spectra at various temperatures. For the spectra at lower temperatures the proximal methylene signals occur around 60 ppm, the distal methylene signals at 35–40 ppm, and the W–CH_3 signals at 25–30 ppm. Chemical shifts are measured downfield from TMS and the solvent is toluene-d_8.

steric factors cannot be ignored, since a change from NMe_2 to NEt_2 groups occurs and the Cl atom has a smaller van der Waals radius and is farther from the W atom than the CH_3 group. These changes would perhaps be conducive to the same trend in bond lengths.

The smaller van der Waals radius of Cl compared to that of CH_3 may be important in accounting for the fact that in solution we observe only the anti rotamer of $W_2Cl_2(NEt_2)_4$, whereas the $W_2Me_2(NEt_2)_4$ compound exists as an equilibrium mixture of comparable proportions of both anti and gauche rotamers. Solvation differences may also influence this distribution of rotamers. This point requires further study.

The comparison made above between observed and calculated differences in the W–CH_3 and W–N bond lengths finds a parallel in the recently reported[13] structure of $(\eta^5$-$C_5H_5)_2Ta(CH_2)(CH_3)$, where the Ta–CH_3 and Ta–CH_2 distances differ by 0.22 Å, while the sp^3 and sp^2 radii for carbon differ by only 0.03 Å. Certainly the additional 0.19-Å shortening can be attributed to Ta–C π bonding to the CH_2 group.

Nuclear Magnetic Resonance Spectra. ^{13}C Spectra. The carbon-13 spectra are shown in Figures 2 and 3. The methylene and W–CH_3 resonances are seen in Figure 2, while the NCH_2–CH_3 resonances are shown in Figure 3.

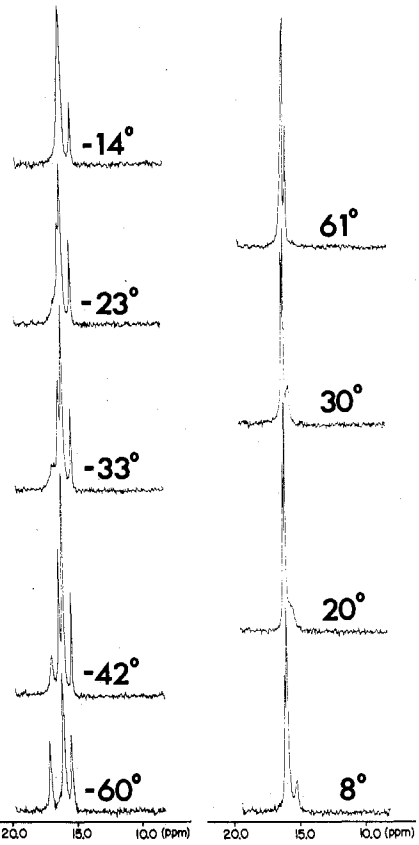

Figure 3. Carbon-13 NMR spectra at various temperatures for the methyl carbon atoms of the ethyl groups. Chemical shifts are measured downfield from TMS and the solvent is toluene-d_8.

The room temperature (30 °C) spectrum of $W_2Me_2(NEt_2)_4$ does not show any sharp resonances attributable to the methylene carbon atoms. It shows an unsymmetrical multiplet for the methyl carbon atoms of the ethyl groups. Its only sharp, unambiguous features are two singlets, with relative intensities of about 3:2 in the region where the W–CH_3 methyl resonances of the anti and gauche rotamers could be expected. Thus it was immediately evident that spectra at both higher and lower temperatures would be required to sort out the structural and dynamical properties of this compound in solution.

Upon cooling of the sample to −60 °C a portion of the solute crystallized out and the spectrum assumed a relatively simple appearance. Only one of the two singlets attributable to W–CH_3 carbon atoms is still clearly observed, $J_{C-^{183}W} = 114$ Hz. Since we know that the anti rotamer is considerably less soluble than the gauche rotamer and that the crystalline compound contains only the anti rotamer, it is reasonable to assume that on cooling of the sample quickly to −60 °C practically all of the anti isomer is precipitated while all or most of the gauche form remains in solution and, at this temperature, the gauche form does not convert very rapidly to the anti form. Thus, the −60 °C spectra shown in Figures 2 and 3 are those of the gauche rotamer with scarcely any anti rotamer observable.

For the gauche rotamer at −60 °C there are peaks at 61.2 (A) and 59.9 (B) ppm for the two kinds (see Figure 4) of proximal methylene carbon atoms, peaks at 38.7 (C) and 37.2 (D) ppm for the two kinds of distal methylene carbon atoms, and a peak at 30.0 ppm for the W–CH_3 carbon atoms. In addition, there are peaks at 16.3 (E) and 15.5 (F) ppm for proximal methyl carbon atoms and peaks at 15.5 (G) and 14.9 (H) ppm for distal methyl atoms. The F and G resonances

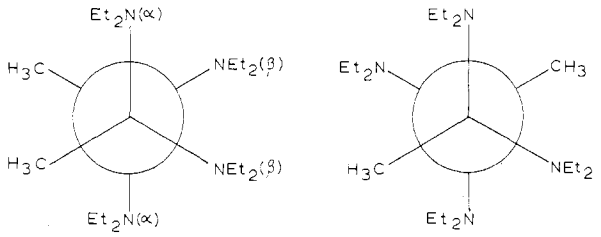

Figure 4. Newman projections of the gauche (left) and anti (right) rotamers of $W_2Me_2(NEt_2)_4$. The nonequivalent NEt_2 groups in the gauche isomer are labeled as α and β.

are superposed. In the spectrum at −42 °C, recorded several hours later, five new lines have appeared in addition to those of the −60 °C spectrum, at 59.3 (I), 38.3 (J), 27.7, 15.8 (K), and 15.5 (L) ppm assignable respectively to the proximal CH_2, distal CH_2, $W-CH_3$, proximal CH_3, and distal CH_3 of the anti rotamer.

In order to analyze the changes in the spectrum which occur from −42 °C to higher temperatures, it is useful to note first that the peaks at 30.0 and 27.7 ppm, due to the $W-CH_3$ groups of the gauche and anti rotamers, respectively, change not at all up to +60 °C. This shows that the gauche–anti (g–a) isomerization rate never attains the NMR time scale in this temperature range and that the g:a isomer ratio does not vary significantly in the temperature range studied.

We turn next to the spectra of the methylene carbon atoms in Figure 2 at temperatures of −42 °C and above. It is clear that peaks B and C have already begun to broaden at −42 °C, whereas peaks A and D have not. This means that proximal–distal exchange proceeds more easily for one pair of NEt_2 groups of the gauche rotamer than for the other. The next pair of peaks to show broadening (beginning at about −23 °C) are those for the anti rotamer (I and J). Finally, at about −14 °C the remaining pair of distal and proximal peaks (A and D) for the gauche rotamer begin to broaden. One would expect to see three close peaks in the fast-exchange limit, two for the two sorts (α and β) of NEt_2 groups of the gauche rotamer and one for the NEt_2 groups of the anti rotamer, with ratios of roughly 3:3:4. However, the highest temperature at which spectra could be recorded without danger of decomposition was 61 °C, where only one broad, unresolved line at the approximate average position for all three pairs of lines is present. The spectra just discussed are thus useful for observations between the slow-exchange limit and the coalescence temperature range but give little information concerning the fast-exchange limit.

Fortunately, the usefulness of the spectra in the methyl region of the ethyl groups is complementary. Because of the small chemical shift differences between the six different signals, the spectrum in the low-temperature region is not very revealing, although it is perfectly consistent with the above interpretation of the spectra in Figure 2. In Figure 3, at −42 °C there are only four resolved lines because three (F, G, L) are superposed in the tallest peak at 15.5 ppm. Already at −42 °C it is apparent that peak E (at 16.3 ppm) is broadening. So also, presumably, is peak F though this is not directly observable since it is part of the large peak at 15.5 ppm. The two peaks E and F can thus be assigned to the methyl groups of the same ethyl groups to which peaks B and C belong, in the gauche rotamer. At about −23 °C it is apparent that peak K at 15.8 ppm, which belongs to an amide methyl group of the anti rotamer, has begun to broaden. Finally at about −14 °C peak H at 14.9 ppm, due to the distal methyl group in the other set of ethyl groups of the gauche rotamer, begins to broaden. All of this is a bit muddled because of the extensive overlapping of resonances. In each case, only one member of the pair that are averaging is clearly seen to broaden because the other member of that pair is in the center of the multiplet and overlaid by other signals. However, at 61 °C it is clear that the expected spectrum for the fast-exchange limit has almost been reached. There are three peaks of comparable intensity. The two sharper ones are due to the averaging processes (E with G; K with L) which began earliest, and the third one, which is not yet fully narrowed at 61 °C, is due to the third averaging process (F with H).

From Figure 2 we can offer some coarse estimates of the relative energies of activation for the three $W-NEt_2$ rotation processes and also make a tentative suggestion as to the relative rates for the α- and β-type NEt_2 groups in the gauche rotamer. It appears that the difference in temperature between comparable degrees of line broadening for the first and the second processes is about 30 °C, while both coalescence temperatures are about 20 °C. If we estimate the two coalescence temperatures to be 5 and 35 °C and also assume that the activation entropies are both equal to zero, it can then be estimated that their activation energies differ by 1.3 ± 0.3 kcal mol^{-1}. In a similar way, it can be estimated that for the third averaging process the activation energy is about another 1.3 kcal mol^{-1} higher. Thus, the activation energies for the two types of NEt_2 group in the gauche rotamer differ by about 2.5 ± 0.5 kcal mol^{-1} while for those in the anti rotamer the value is about halfway between.

^{1}H Spectra. These are more complex and less easily interpreted than the ^{13}C spectra because of the smaller chemical shift differences and consequent overlapping. However, once the general behavior of the system has been deduced from the ^{13}C spectra, the ^{1}H spectra can be interpreted. These spectra not only confirm the interpretation of the ^{13}C spectra but also provide additional information.

Proton spectra at several temperatures are shown in Figure 5. The spectrum at 40 °C in Figure 5a consists of a broad hump at about 3.5 ppm for the methylene protons and a five-line multiplet at about 1 ppm due to the NEt_2 methyl groups and the $W-CH_3$ methyl groups. The two $W-CH_3$ resonances are observed separately because, as shown already by the ^{13}C spectra, g–a interconversion is slow on the NMR time scale. In this spectrum, an equilibrium mixture of anti and gauche isomers is present. The triplet observed for the NEt_2 methyl groups represents the time-averaged proximal and distal methyl groups for both the anti and the gauche rotamers. The chemical shifts are so similar for the two rotamers that the triplets given by each one are superimposed.

On cooling of the sample, the ethyl resonances split into proximal and distal resonances of equal integrated intensity. Since the methylene protons in both anti and gauche rotamers are diastereotopic and since the gauche rotamer contains two pairs of nonequivalent NEt_2 ligands (see Figure 4), we would expect that a low-temperature limiting spectrum of $W_2Me_2(NEt_2)_4$ (one in which the rate of proximal–distal alkyl interchange is slow on the NMR time scale) should consist of six overlapping ABX_3 patterns. The low-temperature limiting spectrum of such a mixture of rotamers is shown in Figure 5b.

Since crystallization of $W_2Me_2(NEt_2)_4$ from alkane solvents yields the pure anti rotamer and since there is a sizable energy of activation for the interconversion of anti and gauche isomers (see later), we have been able to obtain a low-temperature limiting ^{1}H spectrum for the pure or nearly pure anti rotamer. This is shown in Figure 5c and is very similar to that previously reported[4] for $W_2Cl_2(NEt_2)_4$. Attainment of a high-temperature limiting spectrum (fast proximal–distal alkyl exchange) for the pure anti rotamer is not possible because anti–gauche interconversion is fast enough at higher temperatures to restore the gauche–anti equilibrium mixture.

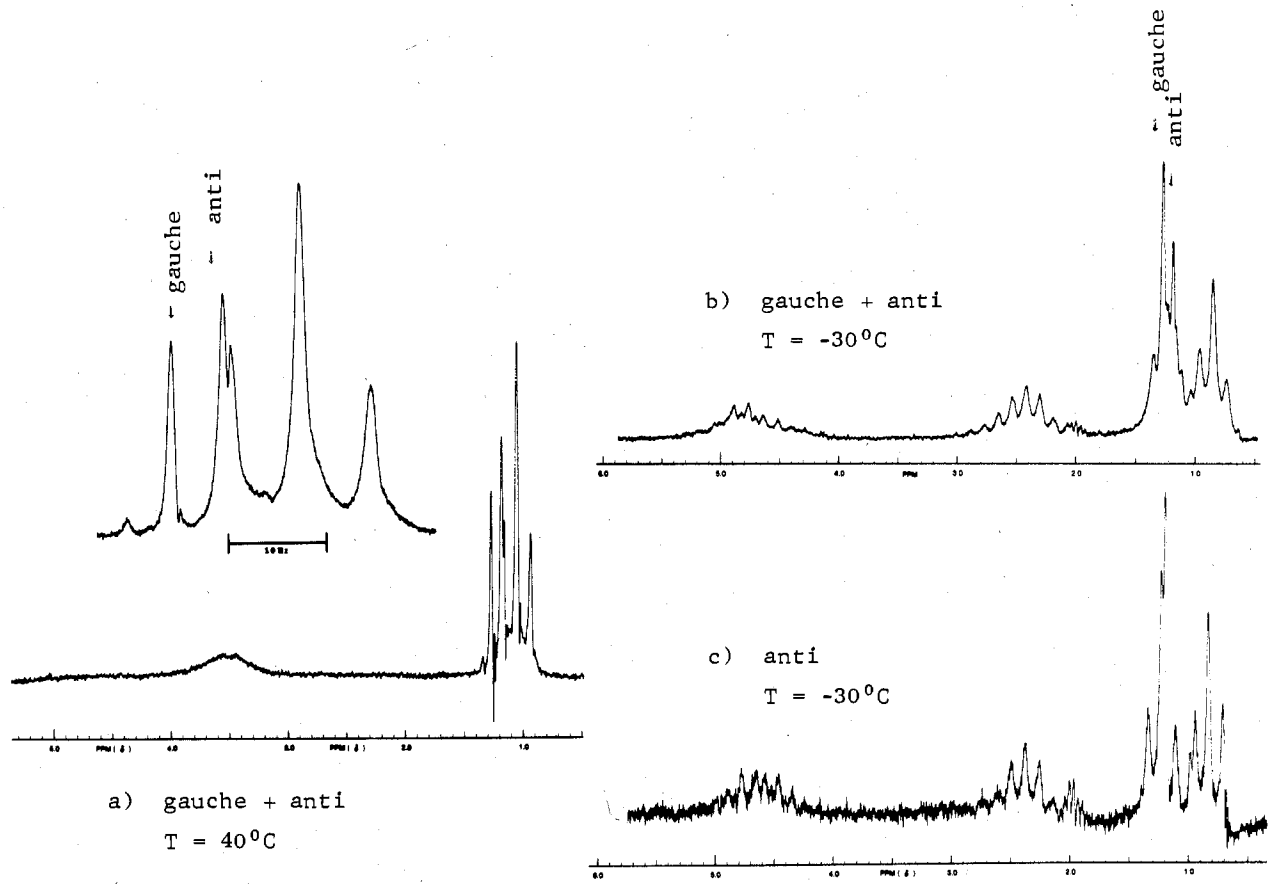

Figure 5. ^{1}H NMR of $W_2(NEt_2)_4Me_2$ at 60 MHz: (a) anti + gauche isomers in benzene (40 °C); (b) anti + gauche isomers in toluene-d_8 (−30 °C); (c) anti isomer in toluene-d_8 (−30 °C).

We have been unable to observe a coalescence of the anti and gauche W-methyl proton resonances. As will be shown below, the activation energy for g–a interconversion is such that coalescence would be expected to occur at ca. 130 °C. At 115 °C separate gauche and anti W–Me resonances are observed, and above this temperature decomposition becomes sufficiently rapid to prevent further observations.

The rate and activation parameters for internal rotation have been investigated in the following way. When the pure solid, which consists entirely of the anti rotamer, is dissolved in toluene-d_8 at about −78 °C, only the anti rotamer is observed, as in Figure 5c. If the sample is then warmed to ca. 10 °C and thermostated in the spectrometer probe at 12 ± 2 °C, the growth of the W–CH_3 peak due to the gauche isomer can be followed as a function of time. Representative spectra are shown in Figure 6. The entire set of measured intensities at different times has been given in the Experimental Section. From an appropriate treatment of these data[14] the rate constant for the anti to gauche rotation is $k_1 = 3.9\ (3) \times 10^{-4}$ s^{-1} at 12 ± 2 °C and $\Delta G_1^{\ddagger}$ is 21.1 (2) kcal mol^{-1}. From an equilibrium constant, [gauche]/[anti] = 1.5, we find $k_{-1} = 2.6\ (2) \times 10^{-4}$ s^{-1} and $\Delta G_{-1}^{\ddagger} = 21.3$ (2) kcal mol^{-1} (where the subscript −1 refers to the gauche → anti process).

Thus, the barrier to rotational interconversion of gauche and anti forms is about 21 ± 1 kcal mol^{-1} if we assume that $\Delta S^{\ddagger}$ is about zero. On the basis of this result, the estimate quoted above that coalescence of the W–CH_3 proton resonances could not be expected below about 130 °C was made. The barrier for gauche to gauche interconversion remains unknown.

A triple bond consisting of a σ component and two equivalent π components has cylindrical symmetry and imposes no restriction on rotation. In view of the similar geometrical properties of M_2L_6 molecules and substituted ethanes a comparison with barriers to rotation about sp^3–sp^3 carbon–carbon single bonds seems pertinent. For the sterically congested ethanes $CMeBr_2$–CMe_2Br, $CMeCl_2$–$CMeCl_2$, and $CMeBr_2$–$CMeBr_2$ barriers of 12.6, 13.5, and 16.6 kcal mol^{-1}, respectively, have been reported.[15] These are some of the highest known barriers to rotation about simple carbon–carbon single bonds. In view of the greater length of the W≡W bond (ca. 2.3 Å vs. ca. 1.5 Å for the C—C bond), the higher barrier in $W_2Me_2(NEt_2)_4$ is all the more noteworthy. However, this comparison fails to take account of the size and shape of the R_2N groups. Even in the staggered conformation of the molecule, in which the R groups are interleaved, there appears to be significant repulsion which results in the W–N–C(proximal) angles being opened to 132.2° while the W–N–C(distal) angles are compressed to an average of 112.3°. In an eclipsed conformation it is clear that even with optimal angles of rotation about the W–N bonds, sizable repulsions would be encountered.

In comparing rotation about the W≡W bond with that about C—C single bonds, it is instructive to consider the substituted triptycenes, where the bridging phenyl groups are somewhat similar in steric character to the R_2N groups and are held rigidly parallel to the C–C axes. For triptycenes, the observed barriers are much higher than in the more conventional substituted ethanes mentioned earlier, ranging from 16 to 37 kcal mol^{-1}, depending on substituents.[16,17] We do not believe that a barrier of about 21 kcal mol^{-1} for rotation about the W≡W bond in $W_2Me_2(NEt_2)_4$ is unreasonable in view of the above considerations. We stress, however, that it would be premature to conclude that this first, and so far only, measured barrier to rotation about the metal-to-metal triple bond in this type of compound is necessarily representative.

Mechanism of Proximal–Distal Alkyl Exchange. This process is readily observed in the NMR spectra of all M_2-

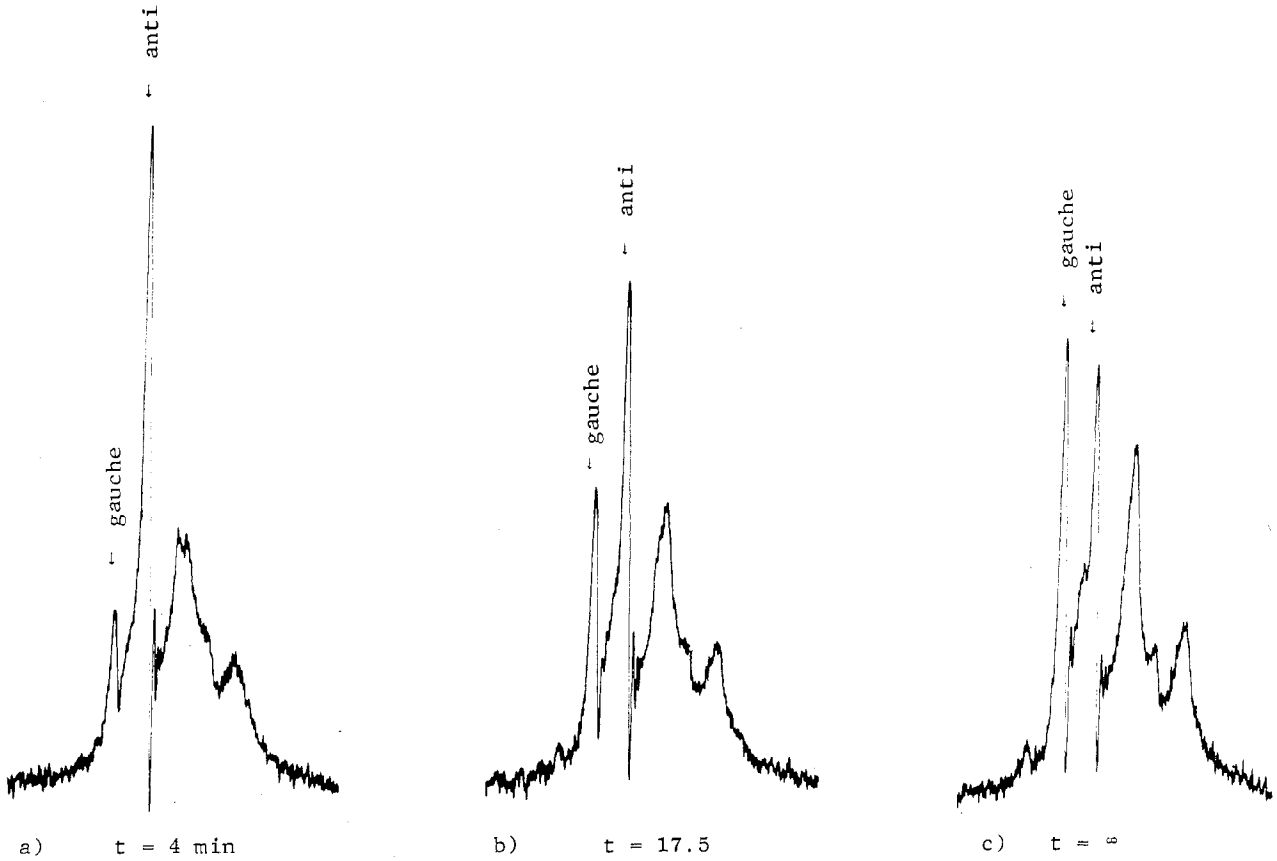

Figure 6. Anti ⇄ gauche isomerization of $W_2(NEt_2)_4Me_2$ in toluene-d_8 at 12 ± 2 °C (followed via ^1H NMR at 60 MHz): (a) $t = 4$ min (ca. 10% gauche); (b) $t = 17.5$ min (ca. 30% gauche); (c) $t = \infty$ (ca. 60% gauche).

$(NR_2)_6$ and $M_2X_2(NR_2)_4$ molecules because of the very large difference in chemical shifts for proximal and distal groups caused by the diamagnetic anisotropy of the M≡M bonds.[2,18] Mechanisms which might be considered for this interconversion process are of the following classes: (i) dissociative processes, i.e., reversible dissociation of NR_2 ligands or reversible cleavage of the M–M bond; (ii) associative processes, including catalysis by free amine; (iii) fluxional processes in which NR_2 groups are transferred via bridge positions between metal atoms, as in the well-documented phenomenon of CO ligand scrambling in polynuclear metal carbonyl complexes;[19] (iv) processes involving "rotations" about metal–nitrogen bonds. Because rotation about an M–N bond axis by one of the NR_2 ligands will be sensed by the other $(n - 1)$ NR_2 groups, the motions of all NR_2 groups in the molecule will be coupled and none of the NR_2 groups will move independently. This type of sympathetic motion in molecular propellers has been called[20] "correlated rotation".

On the basis of the following observations we consider the associative and dissociative reaction pathways to be very unlikely. The rate of proximal–distal alkyl exchange is independent of the concentration of the metal complex and unaffected by added amine. Isotopic labeling studies[21] have shown that $M_2(NMe_2)_6$ molecules do not undergo amine-exchange reactions or metal–metal bond metathesis reactions. It then remains to discriminate between mechanisms of types (iii) and (iv). By consideration of the observed dynamical solution behavior of $W_2X_2(NEt_2)_4$, where X = Cl or Me, we believe a distinction is possible if certain reasonable assumptions are made.

Activation parameters for proximal–distal alkyl exchange in $M_2(NR_2)_6$ and $W_2X_2(NEt_2)_4$, where X = Cl or Me, are given in Table V. The values of $\Delta G^{\ddagger}$ are very similar for all of these compounds which leads us to believe that the mechanism is fundamentally similar in all.

Table V. Activation Parameters for Proximal and Distal Alkyl Exchange in $M_2(NR_2)_6$ and $W_2X_2(NEt_2)_4$ (X = Me, Cl)

Compd	$\Delta\nu$,[a] Hz	T_c, °C	$\Delta G^{\ddagger}$, kcal mol^{-1}
$Mo_2(NMe_2)_6$	108	−30 ± 2	11.5 ± 0.2
$W_2(NMe_2)_6$	113	−35 ± 2	11.2 ± 0.2
$Mo_2(NEt_2)_6$[b]	150	16 ± 5	13.6 ± 0.4
$W_2(NEt_2)_6$[b]	150	10 ± 5	13.3 ± 0.4
$W_2(NEt_2)_4Me_2$[b,c] (i)	147	10 ± 5	13.3 ± 0.4
(ii)	147	39 ± 5	14.7 ± 0.4
$W_2(NEt_2)_4Cl_2$[b]	145	39 ± 5	14.7 ± 0.4
$W_2(NEt_2)_4(NMe_2)_2$[d] (i)	112	−27 ± 5	11.6 ± 0.4
(ii)[b]	144	−10 ± 10	12.3 ± 0.4

[a] $\Delta\nu = \nu$(distal) − ν(proximal) at 60 MHz. [b] $\Delta\nu$ and T_c refer to methylene protons. [c] See text for discussion of ^{13}C NMR studies. [d] (i) NMe_2 exchange. (ii) NEt_2 exchange.

For fluxional processes via bridged intermediates, we suggest that only mechanisms involving the concerted pairwise interchange of NR_2 need be considered. We discount mechanisms leading to the net unsymmetrical transference of NR_2 groups (i.e., $L_3M{\equiv}ML_3 \rightleftarrows L_2M{\equiv}ML_4$) on both steric and electronic considerations. Symmetrical, doubly bridged intermediates $L_2M(\mu\text{-}L)_2ML_2$ are in keeping with the known structural chemistry of a great many compounds, including halides such as $(AlCl_3)_2$ and $(FeCl_3)_2$ and *RS*-bridged species of many kinds, and even have precedents in the specific area of metal amide chemistry, as, for example, in the structure of $Al_2(NMe_2)_6$.[22]

For such pairwise exchange mechanisms,[23] we can then evaluate all four possibilities shown in Figure 7 (where the NR_2 groups exchanged are denoted N′ and the others N) with respect to the following criteria: (1) the diastereotopic nature of the methylene protons of an NEt_2 ligand must be preserved; (2) anti–gauche isomerization must not occur, and (3) all NR_2 groups must be equivalenced. These conditions arise from

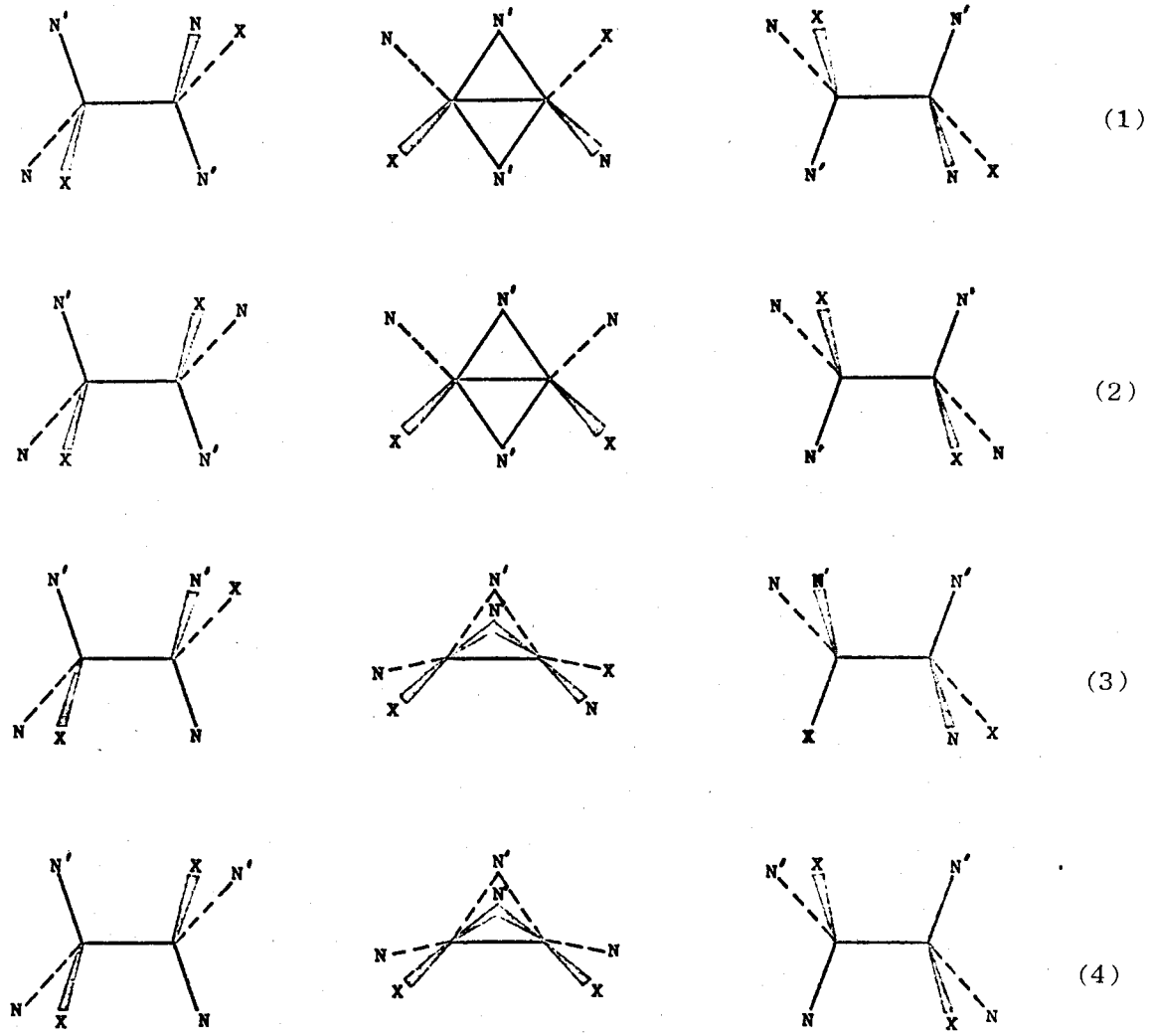

Figure 7. Mechanisms for proximal–distal alkyl exchange involving the concerted pairwise formation of bridges. N′ denotes NR_2 ligands exchanged in this manner.

experimental observations of the dynamical solution behavior of the $W_2X_2(NEt_2)_4$ molecules.

Pathways 1 and 2 in Figure 7 involve the pairwise exchange of trans NR_2 groups. Pathway 1 of the anti rotamer meets all three of the aforementioned conditions, but the analogous pathway 2 for the gauche rotamer equivalences the methylene protons of NEt_2 groups and is selective in providing for proximal–distal alkyl exchange of only a single pair of NEt_2 ligands.

Pathways 3 and 4 involve the pairwise exchange of cis NR_2 ligands. Pathway 3 interconverts anti and gauche isomers and pathway 4 equivalences the AB methylene protons of an NEt_2 ligand.

We conclude that a pairwise exchange of NR_2 ligands via bridged intermediates is not operative for gauche $W_2X_2(NEt_2)_4$, and, from our initial premise that there exists a common type of mechanism, we discount the unique reaction pathway 1 for the anti rotamer.

By a process of elimination, we conclude that proximal–distal exchange in all of the compounds we have studied is accomplished by rotations about the M–N bonds. In view of the steric properties of the NR_2 groups and the $M_2(NR_2)_6$ or $M_2X_2(NR_2)_4$ molecules in their entirety, it is virtually certain that these must be "correlated rotations" in the sense that Mislow[20] used this term. The close stereochemical analogy between the $W_2X_2(NEt_2)_4$ molecules and 1,1,2,2-tetraarylethanes, which have recently been the subject of detailed study,[24] is worth noting. A more detailed discussion of the dynamical behavior of these molecular propellers awaits the characterization of molecules of lower symmetry such as $MX(NR_2)_2MY(NR_2)_2$.

Acknowledgment. We thank the Research Corp., the Petroleum Research Fund, administered by the American Chemical Society, and the National Science Foundation (Grant No. GP42691X) for support of the work at Princeton University and the National Science Foundation (Grant No. GP33142X) for support of the work at Texas A&M University. We thank Professor Kurt Mislow for his interest in the dynamical behavior of this molecule.

Registry No. $W_2(Me)_2(NEt_2)_4$, 59671-97-5; $Mo_2(NMe_2)_6$, 51956-20-8; $W_2(NMe_2)_6$, 54935-70-5; $Mo_2(NEt_2)_6$, 59671-98-6; $W_2(NEt_2)_6$, 57088-64-9; $W_2(NEt_2)_4Cl_2$, 57088-63-8; $W_2(NEt_2)_4(NMe_2)_2$, 59671-99-7; ^{13}C, 14762-74-4.

Supplementary Material Available: Listing of structure factor amplitudes (9 pages). Ordering information is given on any current masthead page.

References and Notes

(1) (a) Princeton University. (b) Texas A&M University.
(2) M. H. Chisholm, F. A. Cotton, B. A. Frenz, W. W. Reichert, L. W. Shive, and B. R. Stults, *J. Am. Chem. Soc.*, **98**, 4469 (1976).
(3) M. H. Chisholm, F. A. Cotton, M. Extine, and B. R. Stults, *J. Am. Chem. Soc.*, **98**, 4477 (1976).
(4) M. H. Chisholm, F. A. Cotton, M. Extine, M. Millar, and B. R. Stults, *J. Am. Chem. Soc.*, **98**, 4486 (1976).
(5) W. Mowat, A. Shortland, G. Yagupsky, N. J. Hill, M. Yagupsky, and G. Wilkinson, *J. Chem. Soc., Dalton Trans.*, 533 (1972); F. Huq, W.

Mowat, A. Shortland, A. C. Skapski, and G. Wilkinson, *Chem. Commun.*, 1079 (1971).
(6) It should be noted that alkoxy compounds $M_2(OR)_6$ are also well-known though none has yet been characterized crystallographically. Cf. M. H. Chisholm and W. Reichert, *J. Am. Chem. Soc.*, **96**, 1249 (1974).
(7) F. A. Cotton, B. A. Frenz, G. Deganello, and A. Shaver, *J. Organomet. Chem.*, **50**, 227 (1973).
(8) Computer programs used in the structural solution and refinement were those of the Enraf-Nonius structure determination package. The software package was used on a PDP 11/45 computer at the Molecular Structure Corp., College Station, Tex.
(9) D. T. Cromer and J. T. Waber, "International Tables for X-Ray Crystallography", Vol. IV, Kynoch Press, Birmingham, England, 1974, Table 2.3.1.
(10) D. T. Cromer and D. Liberman, *J. Chem. Phys.*, **53**, 1891 (1970).
(11) Supplementary material.
(12) V. Schomaker and D. P. Stevenson, *J. Am. Chem. Soc.*, **63**, 37 (1941).
(13) L. J. Guggenberger and R. R. Schrock, *J. Am. Chem. Soc.*, **97**, 6578 (1975).
(14) V. J. Laidler, "Chemical Kinetics", McGraw-Hill, New York, N.Y., 1965, pp 19, 89.
(15) B. L. Hawkins, W. Bremser, S. Borcic, and J. D. Roberts, *J. Am. Chem. Soc.*, **93**, 4472 (1971).
(16) N. M. Sergeyev, K. F. Abdulla, and V. R. Svarchenko, *J. Chem. Soc., Chem. Commun.*, 368 (1972).
(17) M. Iwamura, *J. Chem. Soc., Chem. Commun.*, 232 (1973).
(18) J. San Filippo, Jr., *Inorg. Chem.*, **11**, 3140 (1972).
(19) R. D. Adams and F. A. Cotton in "Dynamic Nuclear Magnetic Resonance Spectroscopy", L. M. Jackman and F. A. Cotton, Ed., Academic Press, New York, N.Y., 1975, p 489.
(20) K. Mislow, *Acc. Chem. Res.*, **9**, 26 (1976).
(21) M. H. Chisholm, M. Extine, and W. W. Reichert, to be submitted for publication.
(22) D. C. Bradley, *Adv. Inorg. Chem. Radiochem.*, **15**, 259 (1972), and references therein.
(23) We have not considered mechanisms involving bridging X groups (X = Cl or Me) since to do so would be against our initial premise that all of these molecules share a common type of mechanism. Furthermore, we note that (i) a pairwise interchange of X groups does not of itself cause proximal–distal alkyl exchange, (ii) a pairwise exchange involving NEt_2 and X generates unsymmetrical species $(NEt_2)_3W{\equiv}WX_2(NEt_2)$, and (iii) the similarity of $\Delta G^{\ddagger}$ for $W_2X_2(NEt_2)_4$ where X = Cl and Me suggests that X bridging mechanisms are not operative.
(24) P. Finocchiaro, W. D. Hounshell, and K. Mislow, *J. Am. Chem. Soc.*, **98**, 4952 (1976).

Contribution from Departments of Chemistry, Princeton University, Princeton, New Jersey 08540, and Texas A&M University, College Station, Texas 77843

The Tungsten–Tungsten Triple Bond. 4.[1] Structural Characterization of Hexakis(trimethylsilylmethyl)ditungsten and Preparation of Bis-μ-(trimethylsilylmethylidyne)-tetrakis(trimethylsilylmethyl)ditungsten

MALCOLM H. CHISHOLM,*[2a] F. ALBERT COTTON,*[2b] MICHAEL EXTINE,[2a] and B. RAY STULTS[2b]

Received March 22, 1976 AIC60201L

The reactions of the trimethylsilylmethyl Grignard reagent with WCl_4 and WCl_6 lead respectively to $W_2(CSiMe_3)_2(CH_2SiMe_3)_4$, **1**, and $W_2(CH_2SiMe_3)_6$, **2**. Compound **1** is an air-sensitive, red-brown solid, extremely soluble, volatile at 120 °C under vacuum, and difficult to crystallize. A structure involving Me_3SiC bridges and a W–W bond is proposed but not proved. Compound **2** was reported earlier by Wilkinson and co-workers. It has now been structurally characterized by x-ray crystallography: space group $P2_1$, a = 12.890 (1) Å, b = 18.546 (2) Å, c = 18.347 (2) Å, β = 109.829 (8)°, V = 4126.1 (8) Å^3, Z = 4. The two crystallographically independent molecules are essentially identical. On the basis of refinement to R_1 = 0.066 and R_2 = 0.083, using 3136 reflections having $I > 3\sigma(I)$ collected with Mo Kα radiation and treating only the tungsten and silicon atoms anisotropically, the following average molecular dimensions were found: W–W = 2.255 Å, W–C = 2.14 Å, Si–C = 2.89 Å, W–W–C = 101.7°. The W_2C_6 skeleton has virtual D_{3d} symmetry. The W–W bond in this compound is the shortest one reported to date and is believed to be of order 3.

Introduction

Though molybdenum and rhenium have provided an abundance of compounds with homonuclear metal-to-metal bonds of high order, tungsten has been much less prolific in this respect.[3] Up to this time no compound with a W–W bond of order 4 has been characterized definitively,[4] although genuine $W_2(O_2CR)_4$ compounds appear to exist in noncrystalline form,[5] despite the fact that such bonds are found in scores of molybdenum compounds.[3] In previous papers we described[1,6,7] the preparation and full structural characterization of several compounds containing unbridged W–W triple bonds, the principal ones being $W_2(NMe_2)_6$, $W_2Cl_2(NEt_2)_4$, and $W_2Me_2(NEt_2)_4$. Prior to that, the only compound reported[8,9] which seemed likely to contain an unbridged W–W triple bond was $W_2(CH_2SiMe_2)_6$. However, this had not been structurally characterized beyond the statement that it is isomorphous with the dimolybdenum analogue, $Mo_2(CH_2SiMe_3)_6$, which had been shown to have an Mo_2C_6 skeleton with D_{3d} symmetry and a Mo–Mo bond length (2.167 Å) consistent with the presence of a triple bond.

In this paper we report the full structural characterization of $W_2(CH_2SiMe_3)_6$ and thereby make possible a comparison of M–M triple bonds in the four related compounds M_2L_6, where M = Mo and W and L = CH_2SiMe_3 and NMe_2. We also report the preparation of a new compound which, on the basis of noncrystallographic evidence, we formulate as bis-μ-(trimethylsilylmethylidyne)-tetrakis(trimethylsilylmethyl)ditungsten, $W_2(CSiMe_3)_2(CH_2SiMe_3)_4$.

Experimental Section

Materials. WCl_6 and $TaCl_5$ were purchased from ROC/RIC and stored in glass ampules (ca. 5–40 g each) under vacuum until needed. $W(CO)_6$ was obtained from Strem Chemical Co. WCl_4 was prepared from the reaction $2WCl_6 + W(CO)_6 \rightarrow 3WCl_4$ in refluxing chlorobenzene and then stored in glass vials under N_2 until needed. Chloromethyltrimethylsilane was purchased from Silar Laboratories, Inc., and stored over molecular sieves until used. The Grignard reagent, Me_3SiCH_2MgCl, was prepared in ether (100% yield assumed) and used immediately. Solvents (pentane, hexane, benzene, toluene, ether, and THF) were dried and freed from dissolved molecular oxygen by distilling from a solution of the solvent, benzophenone, sodium, and phenyl ether (Ph_2O was not added to ether or THF), then stored over CaH_2 under nitrogen until used.

Spectroscopic and Analytical Measurements. Elemental analyses were performed by Alfred Bernhardt Mikroanalytisches Laboratorium, Elbach, West Germany, using drybox sampling techniques.

Infrared spectra were obtained from Nujol mulls between CsI plates using a Beckman IR-12 spectrophotometer.

Mass spectra were obtained using an AEI MS9 mass spectrometer and the direct insertion method (100–120 °C).

^1H and ^{13}C NMR measurements were made on Varian Associates A-60 and CFT20 instruments, respectively. Toluene-d_8 was used as the solvent and chemical shifts are reported as ppm downfield from hexamethyldisiloxane (HMDS) (for ^1H NMR data) or as ppm downfield from TMS (^{13}C NMR data).